

FORTE observations of simultaneous VHF and optical emissions from lightning: Basic phenomenology

D. M. Suszcynsky, M. W. Kirkland, A. R. Jacobson, R. C. Franz, and S. O. Knox

Los Alamos National Laboratory, Space and Atmospheric Sciences Group, Los Alamos, New Mexico

J. L. L. Guillen and J. L. Green

Sensors and Electronics Department, Sandia National Laboratories, Albuquerque, New Mexico

Abstract. Preliminary observations of simultaneous VHF and optical emissions from lightning as seen by the Fast on-Orbit Recording of Transient Events (FORTE) spacecraft are presented. VHF/optical waveform pairs are routinely collected both as individual lightning events and as sequences of events associated with cloud-to-ground (CG) and intracloud (IC) flashes. CG pulses can be distinguished from IC pulses on the basis of the properties of the VHF and optical waveforms but mostly on the basis of the associated VHF spectrograms. The VHF spectrograms are very similar to previous ground-based HF and VHF observations of lightning and show signatures associated with return strokes, stepped and dart leaders, attachment processes, and intracloud activity. For a typical IC flash, the FORTE-detected VHF is generally characterized by impulsive broadband bursts of emission, and the associated optical emissions are often highly structured. For a typical initial return stroke, the FORTE-detected VHF is generated by the stepped leader, the attachment process, and the actual return stroke. For a typical subsequent return stroke, the FORTE-detected VHF is mainly generated by dart leader processes. The detected optical signal in both return stroke cases is primarily produced by the in-cloud portion of the discharge and lags the arrival of the corresponding VHF emissions at the satellite by a mean value of 243 μ s. This delay is composed of a transit time delay (mean of 105 μ s) as the return stroke current propagates from the attachment point up into the region of in-cloud activity plus an additional delay due to the scattering of light during its traversal through the clouds. The broadening of the light pulse during its propagation through the clouds is measured and used to infer a mean of this scattering delay of about 138 μ s (41 km additional path length) for CG light. This value for the mean scattering delay is consistent with the *Thomason and Krider* [1982] model for light propagation through clouds.

1. Introduction

Space-based observations of lightning and thunderstorms in both the radio frequency [e.g., *Herman et al.*, 1965; *Holden et al.*, 1995; *Horner and Bent*, 1969; *Kotaki and Katoh*, 1983; *Leiphart et al.*, 1962; *Massey and Holden*, 1995] and optical [e.g., *Sparrow and Ney*, 1971; *Turman*, 1978; *Vonnegut et al.*, 1983; *Vorpahl et al.*, 1970] parts of the electromagnetic spectrum have been made since the 1960s (see also the review by *Goodman and Christian* [1993]). However, apart from a few brief experiments using the Global Positioning System Nuclear Detonation System (GPS/NDS) in the 1990s and limited use of a fast photodiode in conjunction with the BLACKBEARD very high frequency (VHF) radio experiment aboard the ALEXIS satellite [e.g., *Holden et al.*, 1995], no specifically designed space-based efforts have been mounted to simultaneously observe optical and radio frequency (RF) emissions from lightning on a routine, automated basis. The importance of performing such a study is clear. A dual phenomenology approach to lightning observations from space might significantly contribute to our eventual ability to monitor and remotely identify

lightning types (cloud to ground, intracloud, etc.) from satellites. This has significant implications for planned NASA missions to eventually monitor lightning activity from geosynchronous orbit [*Goodman et al.*, 1988; *Christian et al.*, 1989]. In addition, dual RF/optical observations of lightning from satellites can also provide unique data sets from which to study the basic physics of lightning on a global scale.

In remedy of this situation the Fast on-Orbit Recording of Transient Events (FORTE) satellite was launched on August 29, 1997. FORTE is a joint Los Alamos National Laboratory and Sandia National Laboratories satellite experiment that was primarily designed to address technology issues associated with treaty verification and the monitoring of nuclear tests from space. The satellite carries VHF broadband radio receivers and an Optical Lightning System (OLS) which are optimally designed for the detection of lightning transients. The design of this instrumentation and its availability for continuous scientific use makes FORTE an ideal space platform from which to monitor and study the simultaneous emission of VHF and optical radiation from lightning.

This paper reports on the preliminary phenomenology and analysis of the correlated FORTE VHF and optical data sets. The goals of this study are twofold: (1) to demonstrate the utility of using a dual phenomenology approach for the remote

Copyright 2000 by the American Geophysical Union.

Paper number 1999JD900993.
0148-0227/00/1999JD900993\$09.00

identification of lightning types from space (cloud to ground versus intracloud) and (2) to use the unique perspective of the FORTE data set to study basic lightning emission processes, the effects of clouds on the propagation of light transients, and general lightning phenomenology at the global level.

This paper is organized as follows: Following the introduction in section 1, section 2 provides a brief description of the instrumentation used for the study. The experimental results are described in section 3. Section 3.1 presents the basic phenomenology of simultaneous VHF and optical emissions from lightning as observed by FORTE. Examples of cloud-to-ground (CG) and intracloud (IC) flashes are shown. Section 3.2 defines what is meant by correlation time, scattering delay, and physical delay and details the technique that was used to measure/estimate each quantity. Measurements of these quantities using a 237-event study set are presented as histograms. Section 3.3 presents the results of an effort to estimate the rate of occurrence of detecting VHF/optical waveform pairs. Section 4 discusses the results of section 3 with an emphasis on comparisons to models and previous results.

2. Instrumentation

FORTE is located in a nearly circular, 70° inclination orbit of ~825 km altitude with an orbital period of about 100 min. The instrumentation used for this study includes the two narrowerband FORTE VHF receivers, as described by *Jacobson et al.* [1999b], and the photodiode detector (PDD) of the FORTE OLS, which is described by *Kirkland et al.* [1998].

The VHF instrumentation consists of two broadband receivers that can each be independently configured to cover a 22 MHz subband in the 26–300 MHz frequency range. For this study, one receiver was chosen to span the 26–48 MHz range, and the other spanned the 118–140 MHz range. The instruments were typically configured to collect 40,960 samples in a 800 μ s record length resulting in a time resolution of 20 ns (sample rate of 50 megasamples/second (MSa/s)). The trigger point in each record allowed for 500 μ s of pretrigger information and 300 μ s of posttrigger information. The record length and pretrigger/posttrigger intervals were chosen to optimize the detection and identification of the VHF lightning emissions. Data collection is triggered off the lower (26–48 MHz) band receiver when the amplitude of its detected signal exceeds a preset noise-riding amplitude threshold in at least five of eight 1 MHz-wide subbands distributed throughout the 22 MHz bandwidth [*Jacobson et al.*, 1999b]. This triggering technique allows the instrument to trigger on and detect weak lightning signatures in the presence of strong interfering man-made carriers. Retriggering can occur after only a few microseconds of delay allowing the instrument to record extended multirecord signals with essentially zero dead time. The “field of view” of the VHF receivers is centered on the subsatellite point and is determined by the antenna pattern; the 3 dB attenuation contour of the antenna response approximates a circle of about 1200 km diameter on the Earth and was chosen to roughly correspond to the 80° field of view of the PDD.

The PDD is a broadband (0.4–1.1 μ m) silicon photodiode detector that collects amplitude versus time waveforms of lightning transients. The instrument has an 80° field of view centered on the subsatellite point. This translates into a footprint of about 1200 km diameter on the Earth for an 825 km altitude orbit. The instrument is typically configured to produce 1.92 ms records with 15 μ s time resolution. The PDD is

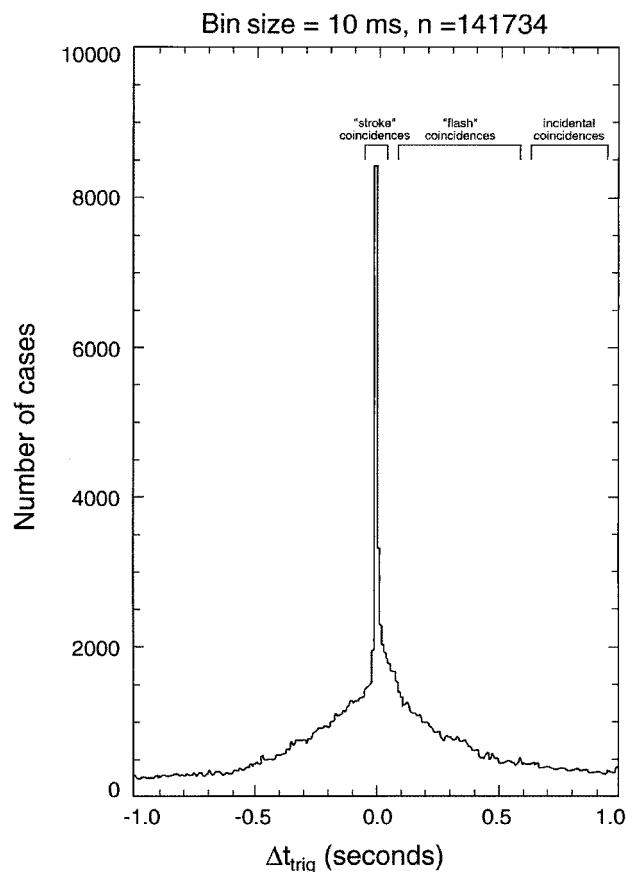


Figure 1. Histogram of VHF/optical trigger time differences, Δt_{trig} , for 141,734 events in the September 5, 1997 to April 15, 1998, time interval.

typically amplitude-threshold triggered, with a noise-riding threshold, and with a requirement that the signal exceed the amplitude threshold for five consecutive samples before a trigger occurs. This protocol eliminates false triggers due to energetic particles. However, the instrument can also be slaved to the VHF receivers, whereby a trigger is forced whenever a VHF signal is received. The PDD provides 12 bit sampling with a piece-wise linear dynamic range covering 4 orders of magnitude and a sensitivity of better than 10^{-5} W/m². Several background compensation modes allow the instrument to be operated both at night and at a reduced sensitivity in the day. There is also a minimum intertrigger delay of about 4.4 ms which results in a ~2.5 ms minimum dead time between successive records. The trigger times of both the VHF and the PDD records are GPS time-stamped to a 1 μ s precision.

3. Observations and Analysis Techniques

3.1. Basic VHF/Optical Phenomenology

Figure 1 contains a histogram of the trigger time differences (i.e., approximate coincidence times), Δt_{trig} , between 141,734 VHF and optical data records that were collected in the September 5, 1997 to April 15, 1998, time period. The VHF receivers and the PDD were operated autonomously during this period, so the coincidence rate between the VHF and the optical triggers was heavily dependent on the triggering and sensitivity biases of each particular instrument. Nonetheless, a

robust collection of time coincidences is apparent. Three classes of coincidences are seen in Figure 1: (1) a narrow and statistically significant population of time coincidences at $\Delta t_{\text{trig}} \sim 0$ s represents correlations between near-simultaneous emissions of VHF and optical radiation from the same lightning pulse (here, the term “pulse” refers to an individual stroke or feature in a multistroke cloud-to-ground (CG) flash, or an individual pulse of radiation from an intracloud (IC) flash made up of many pulses); (2) a broad population of time coincidences in the $0 < |\Delta t_{\text{trig}}| < 0.5$ s time interval that generally represents correlations between the VHF emissions associated with one pulse in a flash and the optical emissions from another pulse in that same flash; and (3) incidental time coincidences in the $|\Delta t_{\text{trig}}| > 0.5$ s regions that are not physically related. For the remainder of the paper we will only consider coincidences (correlations) of the first type in which the VHF and optical radiations are presumably emitted from the same physical event ($\Delta t_{\text{trig}} \sim 0$ s).

An inspection of typical individual correlation cases (Plates 1 and 2) confirms the above interpretation of Figure 1 and demonstrates the basic phenomenology of the VHF/optical correlations. Plate 1a shows a sequence of four consecutive PDD triggers that occur over a 0.25 s time interval. The vertical spikes are actual PDD waveforms that appear compressed because of the large timescale displayed. The red triangles mark the reported times of three strokes of a three-stroke negative CG flash as identified by National Lightning Detection Network (NLDN) data. Plate 1b shows a corresponding sequence of three consecutive low-band VHF waveforms that were collected over the same time interval. The high-band VHF waveforms were generally weaker and less detailed than the low-band waveforms and were, consequently, not used for this study. As can be seen, the FORTE data set captures the majority of the VHF and optical pulses emitted from the NLDN-reported CG flash.

Plates 1c, 1d, and 1e present the detailed comparison of the three VHF/optical pairs in the flash. The black traces show the PDD waveforms, the blue traces show the VHF waveforms, and the red triangles, again, indicate the NLDN-reported return stroke times. The VHF waveforms are displayed on an arbitrary amplitude scale to facilitate time comparisons with the optical waveforms. In each case, the VHF signal is seen to precede the optical signal by tens to a few hundreds of microseconds, depending on how the time delay is measured.

Plates 1f, 1g, and 1h show the VHF spectrograms for the three VHF records displayed in Plates 1c, 1d, and 1e. The spectrograms were generated by taking 256-sample Blackman-windowed fast Fourier transforms of the waveform as the window was moved in 16-sample increments through the record. The spectrograms plot the signal power expressed in dBm (color bar) as a function of frequency and time and show features that are uniquely characteristic of CGs (see section 4). The spectrograms in Plates 1f, 1g, and 1h and their corresponding waveforms in Plates 1c, 1d, and 1e are plotted over the same time intervals in order to facilitate direct comparisons between the two. The arrows in Plates 1f and 1h indicate the NLDN-reported stroke times. The times are corrected for propagation delays to the satellite by using the NLDN source locations, the satellite location, and the WGS84 ellipsoid model of the Earth.

The data are also populated with examples of likely IC flashes, although the NLDN array is generally not useful in validating these examples because of its relative insensitivity to

discharges, which have predominantly horizontal currents. Instead, we identify candidate IC flashes by searching for time intervals (~ 1 – 10 ms) between successive triggers that are characteristic of IC activity. Plate 2 shows an example of a likely IC flash in the same format as Plate 1. Note the 1– 10 ms intervals between many of the pulses. The sequence of pulses was quite isolated in time with no other optical or VHF activity being detected for 3 s before or after the time interval shown. Seven correlated VHF/optical pairs of triggers occurred during the interval; the pairs marked A, B, and C are detailed in Plates 2c–2h. All 18 VHF triggers collected in the time interval were characterized by brief impulsive bursts of VHF such as that shown in Plates 2f, 2g, and 2h. As with the CG example, the VHF signals precede the optical signals by tens to hundreds of microseconds, and the VHF spectrograms show features uniquely characteristic of ICs (see section 4).

3.2. Correlation Time, Scattering Delay, and Physical Delay: Definition and Measurement

The degree to which the VHF signal precedes the optical signal is an important parameter to measure because the delay in the arrival of the optical signal at the satellite can be related to the scattering delay of light as it propagates through the clouds [e.g., *Thomason and Krider*, 1982]. An experimental determination of this number can be used to validate existing light propagation models but is complicated by the fact that the delays may also be influenced by whether or not the observed VHF and optical emissions are both emitted by the same process in the lightning discharge. Unless ground truth is available, it can be difficult to assess this contribution to the total delay.

As a first step in deducing the optical scattering delay due to clouds, a subset of VHF/optical correlation data was analyzed to remove the triggering and thresholding biases introduced by considering trigger time differences (as in Figure 1) rather than true signal arrival time differences (i.e., correlation times). Because of the complex and variable nature of both the VHF and the optical waveforms (see Plates 1 and 2) the true correlation times Δt_{corr} were analyzed and measured by hand, a laborious process that resulted in a much more limited but more physically meaningful data set.

Figure 2 illustrates how the correlation times Δt_{corr} were defined, measured, and related to the scattering delay Δt_{scatt} . We assume that for a generic lightning pulse (e.g., an individual step in a stepped leader, a return stroke in a flash, a dart leader) the VHF emission from the source (driven by changes in current, dI/dt) will precede the emission of light (driven by current, I) by a time no greater than of the order of the risetime of the current pulse (about 1– 10 μ s). This assumption is supported by numerous field experiments [e.g., *Guo and Krider*, 1982; *Ganesh et al.*, 1984; *Beasley et al.*, 1983; *Mach and Rust*, 1993] and laboratory simulations of lightning discharges [e.g., *Gomes and Cooray*, 1998]. In addition, we must allow for any additional physical delay, Δt_{phys} , between the FORTE-detected VHF emission and the FORTE-detected optical emission that would result if the VHF is emitted from one stage of the discharge, and the optical emission is emitted from another stage. Depending on what the sources of the radiations are, Δt_{phys} may have a value of anywhere from a few microseconds (for cases where the detected VHF and optical signals are emitted from the same stage of the discharge) to tens and hundreds of microseconds (for cases where the detected radiations are emitted from different stages of a dis-

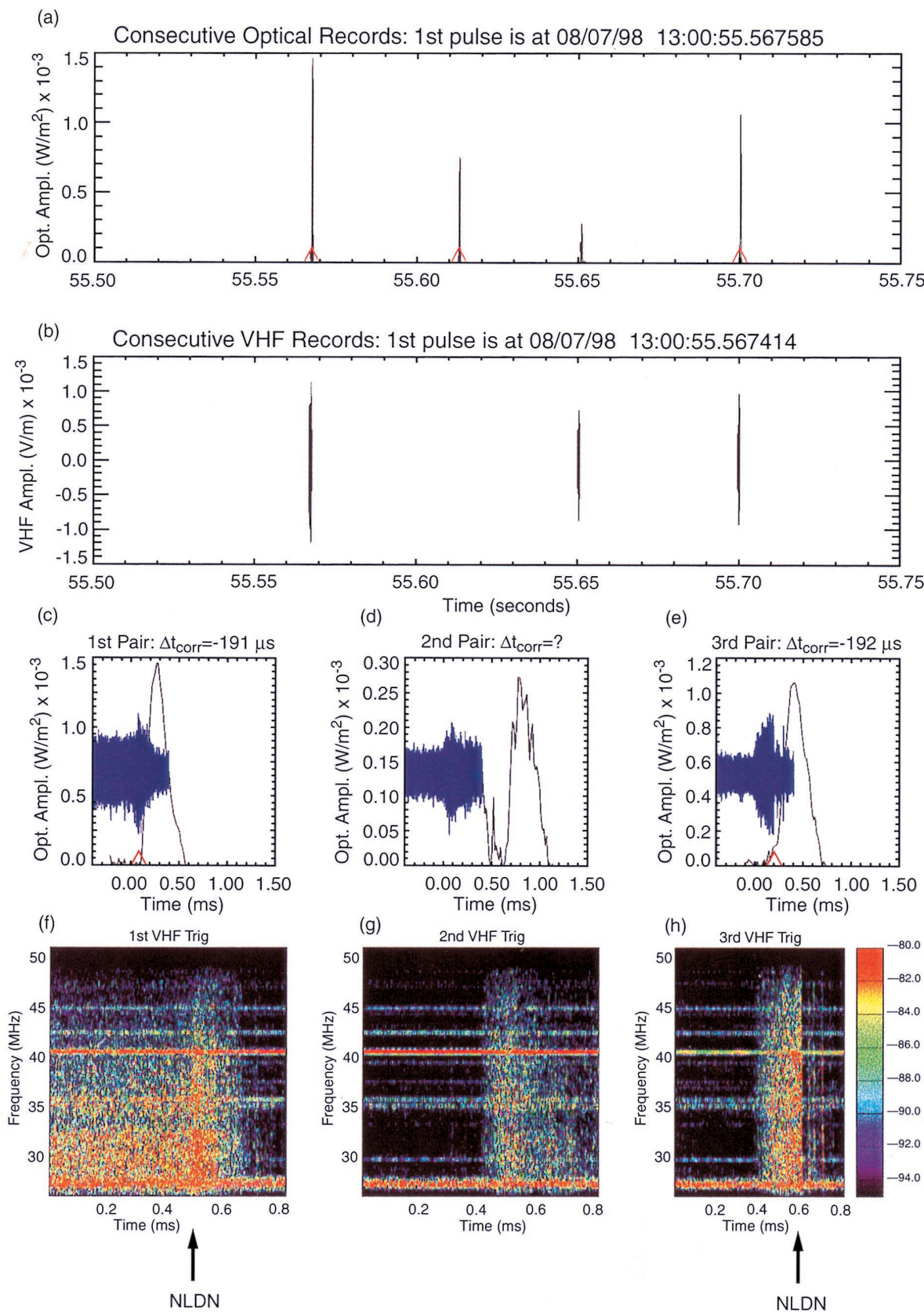


Plate 1. Example of an NLDN-confirmed negative CG flash: (a) consecutive PDD waveforms collected over a 0.25 s time interval with NLDN-detected strokes identified by red triangles; (b) consecutive VHF waveforms collected over the same time interval as in Plate 1a; (c, d, e) expanded plots of the three VHF/optical waveform pairs shown in Plates 1a and 1b; (fgh) frequency-time spectrograms of the three VHF waveforms shown in Plates 1c, 1d, and 1e. The arrows below the spectrograms indicate the NLDN-reported onset times of the return strokes.

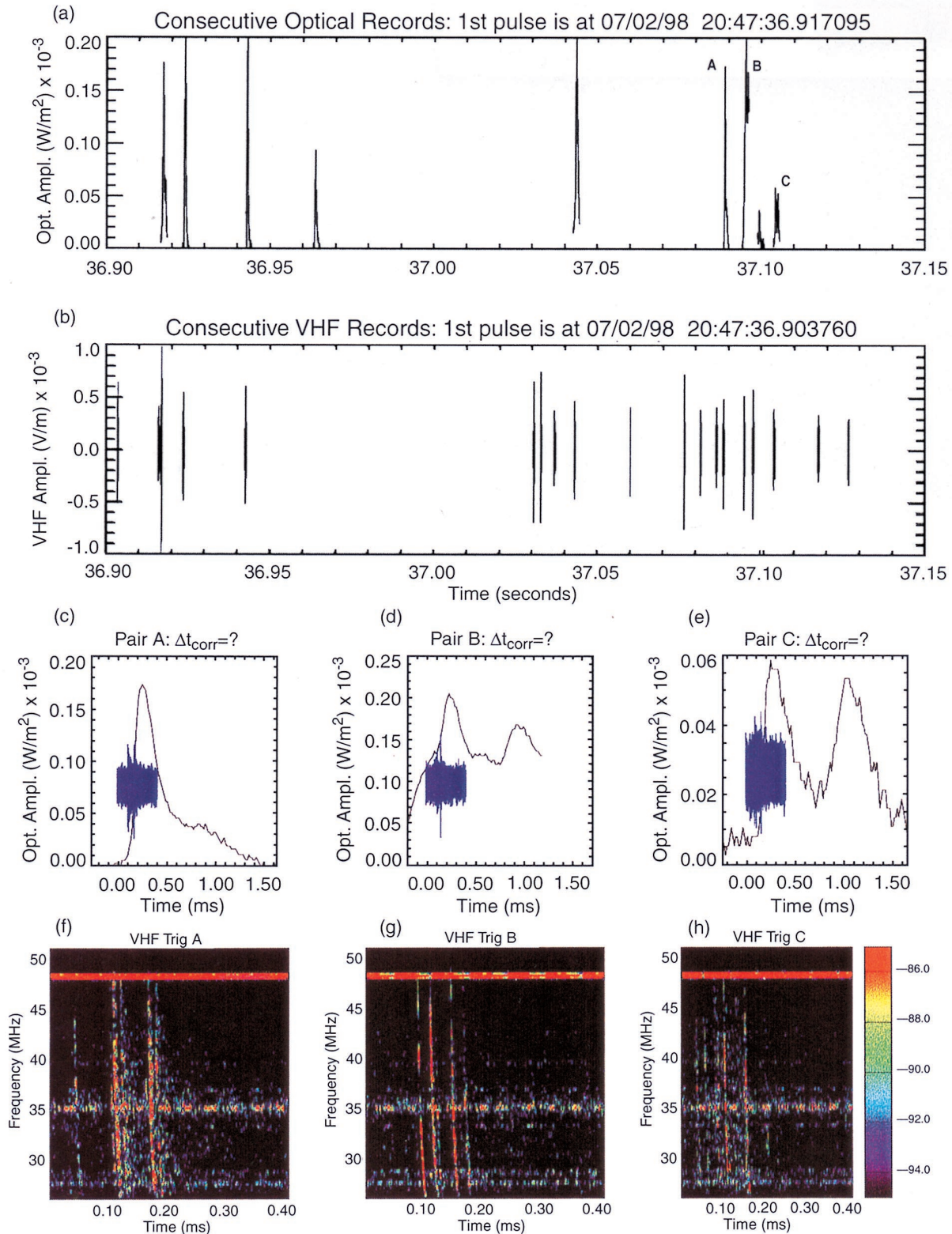


Plate 2. Example of a likely IC flash. Presentation format is the same as that described in Plate 1.

charge). Both radiations then propagate to the satellite with a time delay given by $\Delta t_{\text{prop}} = d/c$, where d is the source-satellite distance, and c is the speed of light. However, the optical signal will acquire an additional delay, Δt_{scatt} , as well as a broadening, both due to the significant Mie scattering that occurs during the light propagation through the clouds.

Δt_{scatt} as well as an estimate for Δt_{phys} can be determined by making two measurements. The first is the “delay measurement” where the time difference of arrival between the VHF signal and the optical signal at the satellite Δt_{corr} is measured and equated to the sum of Δt_{phys} and Δt_{scatt} . For return strokes, Δt_{corr} was determined by measuring the interval be-

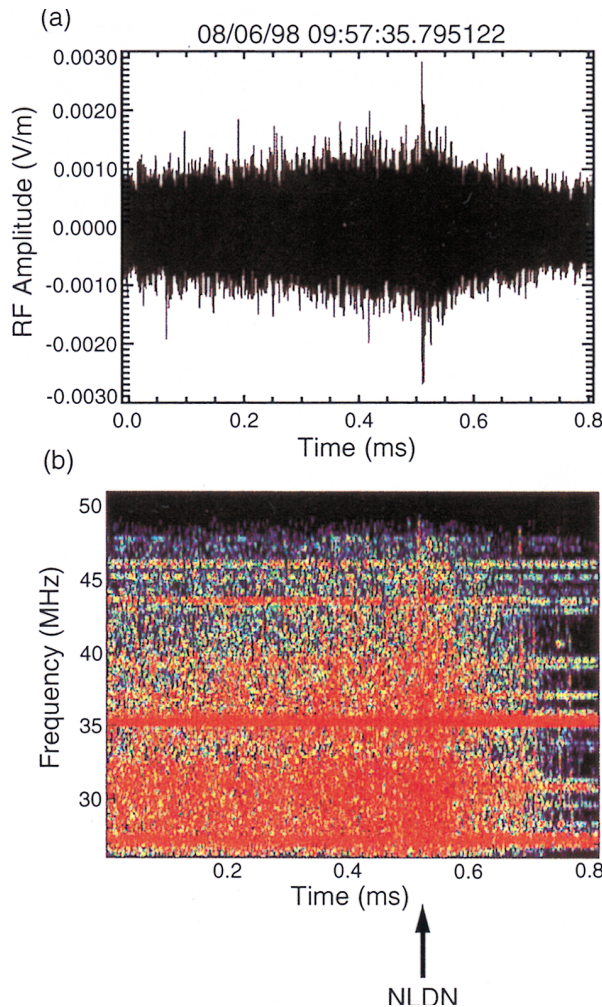


Plate 3. (a) Time waveform and (b) frequency-time spectrogram of an initial return stroke showing an impulsive emission at 500 μ s (arrow) associated with an attachment process.

tween the onset of the return stroke, as determined by the VHF spectrograms and/or NLDN data, and the peak of the associated optical pulse. For IC pulses, Δt_{corr} was determined by measuring the interval between the onset of the impulsive VHF, as determined by the VHF spectrograms and/or NLDN data, and the peak of the associated optical pulse. This method introduces an inherent uncertainty in the measured delay of the order of the risetime of the current pulse (1–10 μ s), but this is small compared to the measured Δt_{corr} values. These measurement points were chosen because they correspond to features in both the VHF and the optical records that are unambiguously identifiable and physically meaningful.

The second measurement is the “broadening measurement” where the broadening of the pulse, or difference between the pulse width at FORTE versus that at the source, $w_F - w_s$, is directly equated to Δt_{scatt} . The convention for measuring the width of an optical pulse is to integrate the full optical waveform over time and then divide by the peak irradiance to arrive at an effective pulse width [Mackerras, 1973]. In this manner, w_F is measured from the PDD waveforms, and w_s is estimated from ground-based measurements of CG activity below the cloud level. Implicit in this technique is the assumption that the broadening of the light pulse due to scattering is equal to the time delay of the light pulse due to scattering. This assumption

is valid as long as the PDD waveforms and the distribution function for the scattering delay of photons propagating through the cloud are fairly symmetric and single-peaked. Both of these requirements are generally met.

The analysis procedure for a given VHF/optical waveform pair, then, is summarized as follows: (1) determine Δt_{scatt} by measuring the amount of optical pulse broadening, (2) measure Δt_{corr} as described above, and (3) then subtract Δt_{scatt} from Δt_{corr} to also arrive at an estimate for Δt_{phys} that can be used to confirm the spectrogram interpretation.

Figure 3 shows a histogram of Δt_{corr} as measured with the above technique for a collection of VHF/optical waveform pairs. The pairs were randomly selected from a 3-week data collection period in July and August 1998 over the continental United States and bordering regions and include the observation of well over 40 storms. VHF record lengths of 800 μ s with 500 μ s of pretrigger time were used to assure that the VHF triggers were of isolated events and not just one small interval of a more extensive emission. The uncertainty in each measurement of Δt_{corr} is estimated to be about ± 50 μ s and reflects uncertainties in the optical time tagging and in properly identifying the start of the return stroke and the peak of the associated optical signal. Of the 264 cases studied, 237 had unambiguous waveforms that allowed Δt_{corr} to be directly measured with the described technique. The 27 ambiguous cases consisted of 14 IC pulses and 13 unidentified pulses and were not measured. The Δt_{corr} values of IC events were generally not measurable because of the difficulty in making a one-to-one correspondence between the complex VHF spectrogram features (see Plates 2f, 2g) and the optical waveform features. The mean value of the 237 Δt_{corr} measurements was -243 μ s, where the minus sign indicates that the VHF signal preceded the arrival of the optical signal at the satellite.

Examples of individual Δt_{corr} measurements for return strokes can be seen in Plate 1. The Δt_{corr} measurements for each of the three VHF/optical pairs are indicated on the tops of Plates 1c, 1d, and 1e. In keeping with measurement convention, a Δt_{corr} for the VHF/optical pair shown in Plate 1d was not measured since the optical peak is ambiguous. The NLDN-reported return stroke onset times are indicated by the arrows below Plates 1f and 1h. The peak times of the optical signals are obvious and not marked. An important observation concerning the 237 measured cases is that 225 (131 confirmed by NLDN and 94 inferred from the spectrogram patterns) were associated with CGs. Of the remaining 12 cases, nine were associated with TIPPps [Holden *et al.*, 1995; Massey and Holden, 1995; Jacobson *et al.*, 1999b] and three were associated with IC pulses.

Figure 3 also contains a second histogram (dashed line) which shows the results of the broadening measurement. To compare this result with the Δt_{corr} measurements, we calculated the effective pulse width for the 237 cases as described above, subtracted 200 μ s, which represents an estimated average effective pulse width for CGs at the source based on the ground measurements of Mackerras [1973] and Guo and Krider [1982], and then took the negative of each result in order to facilitate comparison with the Δt_{corr} histogram. The resulting histogram produces a $\langle \Delta t_{\text{scatt}} \rangle$ (i.e., mean broadening) of about 138 μ s, which equates to a 41 km additional photon path length. We can then calculate $\langle \Delta t_{\text{phys}} \rangle$ as $\langle \Delta t_{\text{phys}} \rangle = \langle \Delta t_{\text{corr}} \rangle - \langle \Delta t_{\text{scatt}} \rangle = 243$ μ s $-$ 138 μ s \equiv 105 μ s. This value of $\langle \Delta t_{\text{phys}} \rangle$ indicates that on the average, there is a 105 μ s delay at the source region between the emission of the VHF radiation

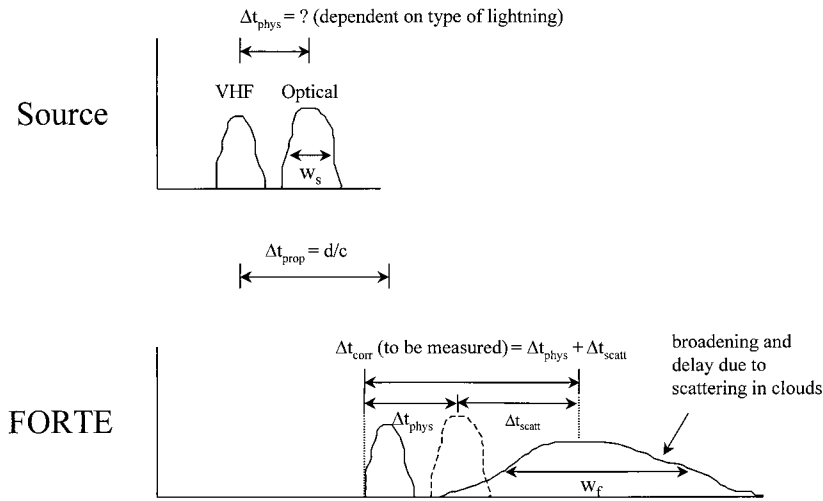


Figure 2. Definition and measurement strategy for Δt_{corr} , Δt_{phys} , and Δt_{scatt} .

detected by FORTE and the emission of the optical radiation detected by FORTE.

The use of a mean effective source pulse width of $200 \mu\text{s}$ in this analysis is not completely justified for the three IC pulses and the nine TIPPAs since this value was based on measurements of CG pulses. However, a more specific value for the mean effective pulse width of an IC pulse at its source is difficult to estimate and has yet to be measured.

3.3. VHF/Optical Correlations: Rate of Occurrence

Finally, measurements were performed to estimate the rate of occurrence of detecting simultaneous VHF/optical triggers from lightning events. An estimate of the rate of correlation between the VHF and optical signals addresses the issue of

using dual phenomenology (VHF plus optical) sensors to execute a satellite-based lightning monitoring mission. With both instruments operating autonomously, as for the data in Figure 1, $\sim 0.2\%$ of the collected VHF lightning events are accompanied by a correlated optical lightning signal, and about 0.4% of the optical lightning events are associated with a correlated VHF lightning signal. These correlation rates are fairly low and result from the fact that each instrument operates independently of the other and is biased by its own triggering and thresholding schemes. Indeed, in the course of normal operations the instruments are typically configured to minimize false alarms at the expense of not detecting the weakest signals.

A controlled experiment was performed to measure a more meaningful occurrence rate by running the PDD in the slave mode, effectively removing all PDD triggering biases. Data were collected over a 4-day period by forcing a PDD trigger whenever the VHF receivers triggered on a lightning event. It was found that 722 VHF lightning triggers out of a total of 6342 events were accompanied by a correlated optical lightning signature giving an occurrence rate of 11.4% , almost 2 orders of magnitude greater than when the instruments were operated autonomously. The nighttime rate was even greater (606 out of 3258 events for a 21.8% correlation rate) and is a result of the higher sensitivity of the PDD in nighttime conditions. These numbers represent a lower limit to the occurrence rate for correlations since the effective field of view of the VHF receivers is significantly larger than that of the PDD.

4. Discussion

4.1. Basic VHF/Optical Phenomenology

The identification of the various lightning features in Plates 1 and 2 is somewhat speculative since adequate ground truth, specifically in the form of radiation waveforms with the proper time resolution, is lacking. The NLDN data offer some ground truth on return strokes although it must be kept in mind that NLDN does not provide waveforms and employs an LF/VLF magnetic field direction-finding system as opposed to the FORTE receivers that measure broadband VHF radiation. No optical ground truth was available for the study. An additional consideration for the detection of CG VHF is that the FORTE antennas will view lightning events from an angle that is sig-

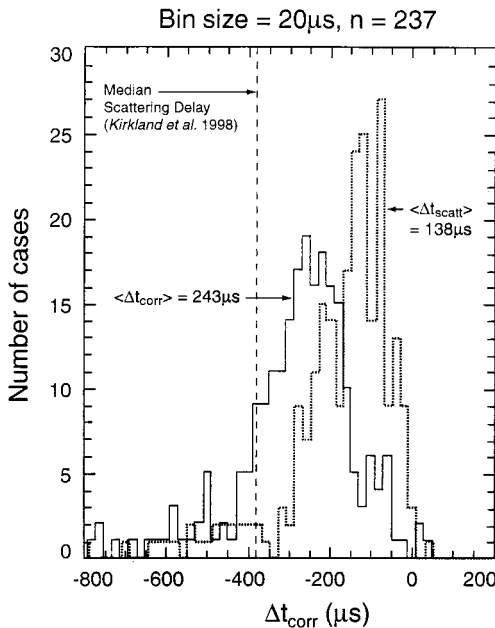


Figure 3. Histograms of Δt_{corr} (solid line) and Δt_{scatt} (dashed line) for 237 VHF/optical correlations. The vertical dotted line at $-380 \mu\text{s}$ represents the median effective scattering delay as measured by Kirkland et al. [1998].

nificantly different than that viewed by a ground-based sensor. Consequently, any directionality in lightning VHF emissions might result in significantly different signatures observed by FORTE as compared to ground sensors. Despite these limitations, the routine association of certain FORTE VHF signatures with certain types of NLDN-verified activity, as is shown in Plate 1, provides us with a good degree of confidence in tentatively assigning interpretations to the features in the spectrograms. This confidence is further supported by striking similarities between the FORTE VHF data and previous ground-based measurements and identifications of HF and VHF emissions from various phases of CG activity [e.g., *Levine and Krider*, 1977; *Hayenga*, 1984; *Rhodes et al.*, 1994; *Shao et al.*, 1995; *Mazur et al.*, 1995].

Plates 1f, 1g, and 1h and Plates 2f, 2g, and 2h contain spectrogram patterns that are typical for those associated with CG and IC flashes. The final interpretation of these types of spectrograms depended on an iterative approach, culminating when a self-consistent analysis was attained among the FORTE VHF and optical observations, the corresponding NLDN data, and the bibliography of previous ground-based interferometer measurements. In the remainder of this section we detail the unique identifying characteristics of each type of lightning displayed in Plates 1 and 2.

The broadband signal in the first 500 μs of the spectrogram in Plate 1f (initial return stroke) is tentatively identified as stepped leader emission. The leader emission is immediately followed by an additional 100 μs burst of radiation that is most likely associated with the actual propagation of the return stroke current. Unlike subsequent strokes, initial return strokes are typically characterized by VHF emissions during the actual return stroke process, presumably related to the characteristic branching of first return stroke channels [e.g., *Levine and Krider*, 1977]. The attachment process presumably occurs at the temporal boundary between the stepped leader and the return stroke. Although not obvious in Plate 1f, the time of attachment is often characterized by an intense, narrow (\sim a few microseconds) burst of VHF such as that shown by the arrow in the example of Plate 3.

To correctly relate the VHF emission to the detected optical emission for first return strokes in the format of Figure 2, we make the assumption that the detected optical signal is associated with the return stroke process and that any optical emissions related to the stepped leader are generally too weak to be detected. This assumption is validated, for example, by the above-cloud aircraft measurements of *Goodman et al.* [1988] in which optical emissions from stepped leaders were rarely measured.

In summary, the identification of first return stroke features is supported by the following observations: (1) the NLDN detection of the onset of the return stroke occurs at the end of the purported leader emission and at the beginning of the burst associated with the return stroke as expected, (2) ground-based interferometer measurements of first return strokes show similar features that agree with those in Plate 1f in terms of the relative intensity and timing of the strokes [e.g., *Rhodes et al.*, 1994; *Shao et al.*, 1995], (3) the time durations of the purported leader (always greater than 500 μs) and return stroke emissions (\sim 100 μs) are consistent with those measured on the ground, (4) VHF emission is detected during the actual return stroke, and (5) as will be seen below, the measured Δt_{corr} , Δt_{scatt} , and Δt_{phys} are consistent with the feature identification.

The two spectrograms shown in Plates 1g and 1h are typical

of subsequent strokes and display an initial interval where the VHF increases in intensity followed by either a steady decrease in intensity (Plates 1d and 1g) or a more common sudden turnoff of emission (Plates 1e and 1h) in coincidence with the onset of the return stroke. The time duration of the entire VHF emission associated with subsequent strokes is typically 100–400 μs . In both spectrograms we identify the entire signal as due to dart leader emission. The gradual turnoff of radiation in Plates 1d and 1g is currently unexplained and is further discussed later in this section.

In summary, the identification of subsequent return stroke features is supported by the following observations: (1) the NLDN detection of the onset of the subsequent return stroke occurs at the end of the purported dart leader emission as expected, (2) ground-based interferometer measurements of subsequent return strokes show similar features that agree with those in Plates 1g and 1h in terms of relative intensity and timing [e.g., *Rhodes et al.*, 1994; *Shao et al.*, 1995], (3) the time durations of the purported dart leader are consistent with those measured on the ground, (4) the cessation of radiation at the onset of the subsequent return stroke is in agreement with ground measurements, and (5) as will be seen below, the measured Δt_{corr} , Δt_{scatt} , and Δt_{phys} are consistent with the feature identification.

The interpretation of subsequent return stroke/dart leader spectrograms (Plates 1g, 1h) is somewhat more difficult than that for initial strokes since their spectrogram signatures are slightly more variable. Dart leaders are strong VHF emitters [e.g., *Hayenga*, 1979; *Levine and Krider*, 1977; *Rhodes et al.*, 1994; *Shao et al.*, 1995] and are known to have a significant optical output that is typically of the order of 10% of that associated with the parent return stroke [*Idone and Orville*, 1985]. Such a signal may be detectable by the PDD but at a much reduced amplitude as compared to the optical emission associated with the actual return stroke current. If optical dart leader signatures were, in fact, detected by the PDD, they would be temporally isolated from the main optical peak associated with the return stroke and easily identified [*Brook et al.*, 1985]. However, nearly all of the optical signatures studied in this paper were single-peaked. Consequently, to correctly relate the detected VHF emission to the detected optical emission for subsequent strokes in the format of Figure 2, we assume that the dart leader optical emission does not significantly contribute to the overall signal detected by the PDD. This assumption is again supported by the measurements of *Goodman et al.* [1988].

The degree to which FORTE detects the various strokes in the flash of Plate 1 is typical of the VHF/optical data set. All three NLDN-reported strokes are accompanied by PDD triggers, while only two of the three strokes registered a VHF trigger. On the other hand, there is a fourth pulse at 55.65 s which was reported by both the VHF and the PDD instruments but was not reported by NLDN. This may simply be a stroke that was missed by the NLDN, or possibly an emission due to a *K* event associated with the flash. *K* events (or *K* changes) often occur in IC flashes and as in-cloud events between successive strokes in a multistroke CG flash and can produce significant optical and VHF radiation (see, for example, the review by *Rakov et al.* [1992]). Indeed, *Goodman et al.* [1988] reported above-cloud observations of *K*-event optical intensities associated with CGs that exceeded those associated with the return strokes. *K* events between return stroke intervals have been equated to dart leaders that do not propagate to

ground and have VHF signatures that are similar to those associated with subsequent return strokes [e.g., Rhodes *et al.*, 1994; Shao *et al.*, 1995]. Consequently, it is likely that some of the “subsequent strokes” included in Figure 3 and identified by their VHF spectrograms rather than by NLDN data are, in fact, between-stroke *K* events/aborted leaders. It is possible that the VHF/optical pair at 55.65 s is due to a *K* event. This might explain why, unlike Plate 1h, there is no sharp cutoff in the VHF emission of Plate 1g. However, at this point, such an identification is pure speculation since we currently have no way to confirm *K* events in the FORTE data set.

The impulsive nature of the VHF spectrogram signals for IC pulses (Plates 2f, 2g, 2h) is presumably related to short multiple bursts of current and is a characteristic signature of FORTE-detected IC pulses [see also Jacobson *et al.*, 1999a]. These signals are TIPP-like [Holden *et al.*, 1995; Massey and Holden, 1995; Jacobson *et al.*, 1999b] in that they are impulsive and are separated by tens of microseconds. However, unlike TIPPS, they occur in multiple pairs, several pairs often occurring within one 800 μ s record. Analogously, the optical waveforms for IC pulses are often broader and more structured than those associated with CG strokes. Given the impulsive, multiple nature of the IC VHF signals seen in Plates 2f, 2g, and 2h, we interpret this optical structure to be due to either (1) multiple optical pulses that are generated by discrete discharge channels developing in quick succession and broadened and coalesced by scattering or (2) optical emissions from one or more discharge channels that are reenergized by repeated surges of current.

The near absence of IC VHF/optical waveform pairs for the data in Figure 3 is unexplained. Again, it is possible that some of the “subsequent strokes” in Figure 3 are actually due to IC *K* events. However, even with this potential misidentification, it is still clear that CGs dominate the data in Figure 3. Given the fact that IC flashes are much more common than CG flashes [Prentice and Mackerras, 1977; Mackerras *et al.*, 1998], this would seem to indicate that the FORTE detection of VHF/optical pairs of waveforms is preferential to CGs. This is in contrast to the result that we find when the FORTE VHF and optical data sets are considered individually [Jacobson *et al.*, 1999; Suszczyński *et al.*, 1999]. In each of these cases, IC detections are more numerous than CG detections. A full analysis and explanation of this observation necessitates a comparison between VHF and PDD triggering biases, source current waveforms, and VHF/optical signal risetimes for CG versus IC pulses and is beyond the scope of this paper.

A more detailed analysis that quantifies the VHF spectrograms and optical signal characteristics for specific types of lightning is ongoing and will be reported on in a subsequent paper. However, it is already clear from this initial analysis that an analysis of VHF signatures of lightning in tandem with optical data can greatly enhance a satellite’s ability to discriminate lightning types from space. Some discrimination information can be found in the optical waveforms: for example, IC waveforms are often broader and more structured than CG waveforms. However, the bulk of the discrimination capability in the FORTE instruments seems to lie in the interpretation of the VHF spectrograms. On the basis of the 131 NLDN-corroborated cases from the data shown in Figure 3, we find that we can distinguish among initial return strokes, subsequent return strokes, and intracloud discharges at a better than 90% confidence level.

4.2. The Δt_{corr} , Δt_{scatt} , and Δt_{phys}

The value for $\langle \Delta t_{\text{phys}} \rangle$ that was deduced from the measurements in Figure 3 can be compared to previous experimental data. Ground-based interferometer measurements indicate that the strongest VHF near the time of initial return strokes occurs during the attachment process and that this emission typically precedes the in-cloud portion of the return stroke by $\sim 100 \mu$ s [e.g., Shao *et al.*, 1995]. Our measurement of $\langle \Delta t_{\text{phys}} \rangle = 105 \mu$ s is in good agreement with this time delay. Likewise, for subsequent strokes the measured $\langle \Delta t_{\text{phys}} \rangle$ is comparable in value to the time delay expected between the initiation of the subsequent return stroke and the optical in-cloud activity that follows. These comparisons imply that the FORTE-detected VHF from CGs is generally produced by below-cloud processes (leaders, attachment processes, and in the case of initial strokes, the actual return stroke), while the FORTE-detected light from CGs is produced by the in-cloud portion of the return stroke. The implication is that in general, return stroke light emissions originating below the cloud deck are scattered to the extent that they fall below the detection threshold of the PDD.

It is important to emphasize that these last two statements have been formulated only for the type of data that we are analyzing in this paper, i.e. for lightning events in which both VHF and optical signals are collected. For example, when looking at only optical/NLDN correlations, we sometimes find what appear to be examples of optical emissions from stepped leaders, dart leaders, and below-cloud portions of return strokes. However, these examples are relatively uncommon. Also, when looking at only VHF/NLDN correlations, the dominant lightning events are TIPPs rather than CGs [Jacobson *et al.*, 1999a].

A comparison between the measured $\langle \Delta t_{\text{scatt}} \rangle$ and the predictions from various cloud-scattering models is generally difficult since the initial conditions of the models do not always match up to the existing conditions during the FORTE measurements. Likewise, the existing cloud and source conditions during the FORTE measurements are not well understood, particularly in the absence of ground truth. However, the measured $\langle \Delta t_{\text{scatt}} \rangle$ of 138 μ s compares favorably to the results of Thomason and Krider [1982]. The Thomason and Krider [1982] model for light propagation through clouds is based on a Monte Carlo method that simulates Mie scattering processes driven by homogenous clouds of various dimensions and particle-size compositions. The model is particularly applicable to the FORTE data set since it considers light scattering and absorption of impulsive point source emissions placed at various locations within finite, geometric clouds. For a light transient located at the center of a cubic cloud of optical depth 200 and water drop diameter of 10 μ m (moderate maritime cumulonimbus) the model predicts a $\langle \Delta t_{\text{scatt}} \rangle$ of about 51 μ s (15 km increased path length), while the predicted value for an optical depth of 400 (strong maritime cumulonimbus) is 130 μ s (39 km increased path length). The $\langle \Delta t_{\text{scatt}} \rangle$ result of Figure 3 compares only generally to the recent measurements of Pfeilsticker *et al.* [1998] which show a scattering delay of the order of 350 μ s for two observed cumulonimbus thunderstorm clouds of 5 km vertical extent. These values were measured for transmission of light from a source above the clouds (the Sun) to the detector below the clouds and tend to significantly overestimate the additional path length that one would expect for a

source near the center of the cloud, as would be the case for IC lightning or the in-cloud components of return strokes.

Kirkland *et al.* [1998] used the full FORTE/PDD data set to estimate a $\langle \Delta t_{\text{scatt}} \rangle$ value greater than $447 \mu\text{s}$ (114 km). Since the Kirkland *et al.* [1998] width distribution was nonnormal, their median value of $\Delta t_{\text{scatt}} = 380 \mu\text{s}$ is the more appropriate value to use for comparisons to this study. This value is marked as a vertical dashed line in Figure 3 and is significantly greater than the $\langle \Delta t_{\text{scatt}} \rangle$ value shown in the histogram of Figure 3. The discrepancy between the Kirkland *et al.* [1998] result and the result of this study is apparently a function of lightning type. Kirkland *et al.* [1998] did not distinguish between CG and IC-produced light. Since IC pulses are the predominant type of lightning and since the IC light signals detected by FORTE are generally broader and more structured than those associated with CGs, the inclusion of IC light in the Kirkland *et al.* [1998] statistics tends to bias the estimate for $\langle \Delta t_{\text{scatt}} \rangle$ to larger values than those associated with just CGs. In fact, when the Kirkland *et al.* [1998] analysis was reapplied to just CG events (4424 NLDN-confirmed cases [Suszcynsky *et al.*, 1999], we calculated a mean effective pulse width of $\sim 203 \mu\text{s}$, much closer to the $138 \mu\text{s}$ value measured for this study.

As a final comment, there is a fair amount of variability in the Mackerras [1973] and Guo and Krider [1982] measurements of the effective pulse width. This variability has a direct impact on our estimates of $\langle \Delta t_{\text{phys}} \rangle$ and $\langle \Delta t_{\text{scatt}} \rangle$. For example, Mackerras [1973] measured 46 return strokes and arrived at a median effective pulse width of $200 \mu\text{s}$ with a large standard deviation, and Guo and Krider [1982] measured 23 strokes for a mean effective pulse width of $158 \mu\text{s} \pm 33 \mu\text{s}$. Given the level of variability seen in these measurements and the difference in experimental techniques between the two studies, we chose not to average the two measurements but to rather just quote the Mackerras [1973] results. This facilitated comparison to the Kirkland *et al.* [1998] measurements that also use the Mackerras [1973] results. Whether we use the Mackerras [1973] results, the Guo and Krider [1982] results, or some (weighted) average of the two, our derived values for $\langle \Delta t_{\text{phys}} \rangle$ and $\langle \Delta t_{\text{scatt}} \rangle$ do not vary by more than a few tens of microseconds, and the basic conclusions of our analysis remain unchanged.

In conclusion, the satellite-based collection of simultaneous VHF and optical emissions from lightning transients is a powerful technique that can be used to study both thunderstorm and lightning processes on a global basis. The preliminary results of this study indicate that we can use VHF/optical correlations to (1) effectively identify and distinguish between CG and IC pulses, including stepped and dart leaders, attachment processes, and return strokes, and (2) estimate a mean scattering delay for the in-cloud portion of CG-emitted light ($138 \mu\text{s}$).

Acknowledgments. The authors would like to thank Paul Krehbiel of The New Mexico Institute of Mining and Technology, and Paul Argo, Anthony Davis, Dott Delapp, Bob Roussel-Dupre, Diane Roussel-Dupre, Ken Eack, Dan Holden, Phil Klingner, Charley Rhodes, Xiaun-Min Shao, and Dave Smith of Los Alamos National Laboratory for useful discussions, comments, and support during this study. This work was supported by the United States Department of Energy.

References

Beasley, W. H., M. A. Uman, D. M. Jordan, and C. Ganesh, Simultaneous pulses in light and electric field from stepped leaders near ground level, *J. Geophys. Res.*, **88**, 8617–8619, 1983.

- Brook, M., C. Rhodes, O. H. Vaughan Jr., R. E. Orville, and B. Vonnegut, Nighttime observations of thunderstorm electrical activity from a high-altitude airplane, *J. Geophys. Res.*, **90**, 6111–6120, 1985.
- Christian, H. J., R. J. Blakeslee, and S. J. Goodman, The detection of lightning from geostationary orbit, *J. Geophys. Res.*, **94**, 13,329–13,337, 1989.
- Ganesh, C., M. A. Uman, W. H. Beasley, and D. M. Jordan, Correlated optical and electric field signals produced by lightning return strokes, *J. Geophys. Res.*, **89**, 4905–4909, 1984.
- Gomes, C., and V. Cooray, Correlation between the optical signatures and current waveforms of long sparks: Applications in lightning research, *J. Electrostat.*, **43**, 267–274, 1998.
- Goodman, S. J., and H. J. Christian, Global observations of lightning, in *Atlas of Satellite Observations Related to Global Change*, Cambridge Univ. Press, New York, 1993.
- Goodman, S. J., H. J. Christian, and W. D. Rust, A comparison of the optical pulse characteristics of intracloud and cloud-to-ground lightning as observed above clouds, *J. Appl. Meteorol.*, **27**, 1369–1381, 1988.
- Guo, C., and E. P. Krider, The optical and radiation field signatures produced by lightning return strokes, *J. Geophys. Res.*, **87**, 8913–8922, 1982.
- Hayenga, C. O., Characteristics of lightning VHF radiation near the time of the return stroke, *J. Geophys. Res.*, **89**, 1403–1410, 1984.
- Herman, J. R., J. A. Caruso, and R. G. Stone, Radio astronomy explorer (RAE-1), observation of terrestrial radio noise, *Planet. Space Sci.*, **21**, 443–461, 1965.
- Holden, D. N., C. P. Munson, and J. C. Devenport, Satellite observations of transionospheric pulse pairs, *Geophys. Res. Lett.*, **22**(8), 889–892, 1995.
- Horner, F., and R. B. Bent, Measurement of terrestrial radio noise, *Proc. R. Soc. A*, **311**, 527–542, 1969.
- Idone, V. P., and R. E. Orville, Correlated peak relative light intensity and peak current in triggered lightning subsequent return strokes, *J. Geophys. Res.*, **90**, 6159–6164, 1985.
- Jacobson, A. R., S. O. Knox, R. Franz, D. C. Enemark, FORTE observations of lightning radio-frequency signatures: Capabilities and basic results, *Radio Sci.*, **34**, 337–354, 1999a.
- Jacobson, A. R., K. L. Cummins, M. Carter, P. Klingner, D. Roussel-Dupre, and S. O. Knox, FORTE observations of lightning radio-frequency signatures: Prompt coincidence with National Lightning Detection Network sferics, *J. Geophys. Res.*, in press, 1999b.
- Kirkland, M. W., D. M. Suszcynsky, R. Franz, J. L. L. Guillen, and J. L. Green, Observations of terrestrial lightning at optical wavelengths by the photodiode detector on the FORTE satellite, Rep. LA-UR-98-4098, Los Alamos Natl. Lab., Los Alamos, N. M., 1998.
- Kotaki, M., and C. Katoh, The global distribution of thunderstorm activity observed by the ionosphere sounding satellite (ISS-b), *J. Atmos. Sol. Terr. Phys.*, **45**, 833–847, 1983.
- Leiphart, J. P., R. W. Zeek, L. S. Bearce, and E. Toth, Penetration of the ionosphere by very low frequency radio signals, Interim results of the LOFTO-I experiment, *Proc. IRE*, **6**, 6–17, 1962.
- Levine, D. M., and E. P. Krider, The temporal structure of HF and VHF radiations during Florida lightning return strokes, *Geophys. Res. Lett.*, **4**, 13–16, 1977.
- Mach, D. M., and W. D. Rust, Two-dimensional velocity, optical rise-time, and peak current estimates for natural positive lightning return strokes, *J. Geophys. Res.*, **98**, 2635–2638, 1993.
- Mackerras, D., Photoelectric observations of the light emitted by lightning flashes, *J. Atmos. Sol. Terr. Phys.*, **35**, 521–535, 1973.
- Mackerras, D., M. Darveniza, R. E. Orville, E. R. Williams, and S. Goodman, Global lightning: Total, cloud, and ground flash estimates, *J. Geophys. Res.*, **103**, 19,791–19,809, 1998.
- Massey, R. S., and D. N. Holden, Phenomenology of transionospheric pulsed pairs, *Radio Sci.*, **30**(5), 1645–1659, 1995.
- Mazur, V., P. R. Krehbiel, and X. M. Shao, Correlated high-speed video and radio interferometric observations of a cloud-to-ground lightning flash, *J. Geophys. Res.*, **100**, 25,731–25,753, 1995.
- Pfeilsticker, K., F. Erle, O. Funk, L. Marquard, T. Wagner, and U. Platt, Optical path modifications due to tropospheric clouds: Implications for zenith sky measurements of stratospheric gases, *J. Geophys. Res.*, **103**, 25,323–25,335, 1998.
- Prentice, S. A., and D. Mackerras, The ratio of cloud to cloud-ground lightning flashes, I, Thunderstorms, *J. Appl. Meteorol.*, **16**, 545–550, 1977.

- Rakov, V. A., R. Thottappillil, and M. A. Uman, Electric field pulses in *K* and *M* changes of lightning ground flashes, *J. Geophys. Res.*, **97**, 9935–9950, 1992.
- Rhodes, C. T., X. M. Shao, P. R. Krehbiel, R. J. Thomas, and C. O. Hayenga, Observations of lightning phenomena using radio interferometry, *J. Geophys. Res.*, **99**, 13,059–13,082, 1994.
- Shao, X. M., P. R. Krehbiel, R. J. Thomas, and W. Rison, Radio interferometric observations of cloud-to-ground lightning phenomena in Florida, *J. Geophys. Res.*, **100**, 2749–2783, 1995.
- Sparrow, J. G., and E. P. Ney, Lightning observations by satellite, *Nature*, **232**, 540–541, 1971.
- Suszcynsky, D. M., M. Kirkland, P. Argo, R. Franz, A. Jacobson, S. Knox, J. Guillen, J. Green, and R. Spalding, Thunderstorm and lightning studies using the FORTE optical lightning system (FORTE/OLS), in *Proceedings of the 11th International Conference on Atmospheric Electricity*, edited by H. Christian, *NASA/CP-1999-209261*, pp. 672–675, 1999.
- Thomason, L. W., and E. P. Krider, The effects of clouds on the light produced by lightning, *J. Atmos. Sci.*, **39**, 2051–2065, 1982.
- Turman, B. N., Analysis of lightning data from the DMSP satellite, *J. Geophys. Res.*, **83**, 5019–5024, 1978.
- Vonnegut, B., O. H. Vaughan, and M. Brook, Photographs of lightning from the space shuttle, *Bull. Am. Meteorol. Soc.*, **64**, 150–151, 1983.
- Vorpahl, J. A., J. G. Sparrow, and E. P. Ney, Satellite observations of lightning, *Science*, **169**, 860–862, 1970.
-
- R. C. Franz, A. R. Jacobson, M. W. Kirkland, S. O. Knox, and D. M. Suszcynsky, Los Alamos National Laboratory, Space & Atmospheric Sciences Group, MS D466, Los Alamos, NM 87545. (dsuszcynsky@lanl.gov)
- J. L. Green and J. L. L. Guillen, Sandia National Laboratories, Sensors and Electronics Dept., MS 0972, Albuquerque, NM 87185.

(Received April 23, 1999; revised September 9, 1999; accepted September 15, 1999.)

